Chiral Symmetry and Low-Energy Pion-Photon Reactions

Norbert Kaiser[1]
Physik-Department T39
Technische Universität München
D-85747 Garching, GERMANY

This talk reviews the description of low-energy pion Compton scattering $\pi^-\gamma \to \pi^-\gamma$ and (neutral/charged) pion-pair production $\pi^-\gamma \to \pi^-\pi^0\pi^0/\pi^+\pi^-\pi^-$ at next-to-leading order in chiral perturbation theory. The first process allows one to extract the pion electric and magnetic polarizabilities (α_π and β_π), while the second reaction is governed by the chiral pion-pion interaction. In addition to the strong interaction effects from chiral loops and counterterms, the QED radiative corrections to these processes are also studied. The predictions of chiral perturbation theory will be tested by the COMPASS experiment at CERN. In case of the total cross section for $\pi^-\gamma \to \pi^+\pi^-\pi^-$ in the near threshold region $\sqrt{s} < 5m_\pi$ a recent analysis of the COMPASS data nicely confirms the prediction of chiral perturbation theory.

1 Introduction and summary

The pions (π^+, π^0, π^-) are the Goldstone bosons of spontaneous chiral symmetry breaking in QCD: $SU(2)_L \times SU(2)_R \to SU(2)_V$. Their low-energy dynamics can therefore be calculated systematically (and accurately) with chiral perturbation theory in form of a loop-expansion based on an effective chiral Lagrangian. The accurate two-loop prediction [1] for the isospin-zero S-wave $\pi\pi$-scattering length $a_0 = (0.220 \pm 0.005)m_\pi^{-1}$ has been confirmed in the E865 [2] and NA48/2 [3] experiments by analyzing the $\pi^+\pi^-$ invariant mass distribution of the rare kaon decay mode $K^+ \to \pi^+\pi^-e^+\nu_e$. One particular implication of that good agreement between theory and experiment is that the quark condensate $\langle 0|\bar{q}q|0\rangle$ constitutes the dominant order parameter [4] of spontaneous chiral symmetry breaking (considering the two-flavor sector of QCD). Likewise, the DIRAC experiment [5] has been proposed to determine the difference of the isospin-zero and isospin-two S-wave $\pi\pi$-scattering lengths $a_0 - a_2$ by measuring the life time ($\tau \simeq 3\,\mathrm{fs}$) of pionium (i.e. $\pi^+\pi^-$ bound electromagnetically and decaying into $\pi^0\pi^0$). In the meantime the NA48/2 experiment [6] has accumulated very high statistics for the charged kaon decay modes $K^\pm \to \pi^\pm\pi^0\pi^0$, which allowed to

[1] nkaiser@ph.tum.de

extract the value $a_0 - a_2 = (0.257 \pm 0.006)m_\pi^{-1}$ for the $\pi\pi$-scattering length difference from the cusp effect in the $\pi^0\pi^0$ mass spectrum at the $\pi^+\pi^-$ threshold. This experimental result is again in very good agreement with the two-loop prediction $a_0 - a_2 = (0.265 \pm 0.004)m_\pi^{-1}$ of chiral perturbation theory [1]. For a discussion of isospin breaking corrections which have to be included in a meaningful comparison between theory and experiment, see ref. [7]. Clearly, these remarkable confirmations give confidence that chiral perturbation theory is the correct framework to calculate reliably and accurately the strong interaction dynamics of the pions at low energies.

Electromagnetic processes offer further possibilities to probe the internal structure of the pion. For example, pion Compton scattering $\pi^-\gamma \to \pi^-\gamma$ at low energies allows one to extract the electric and magnetic polarizabilities (α_π and β_π) of the charged pion. Chiral perturbation theory at two-loop order gives for the dominant pion polarizability difference the firm prediction $\alpha_\pi - \beta_\pi = (5.7 \pm 1.0) \cdot 10^{-4}\,\mathrm{fm}^3$ [8]. It is however in conflict with the existing experimental results from Serpukhov $\alpha_\pi - \beta_\pi = (15.6 \pm 7.8) \cdot 10^{-4}\,\mathrm{fm}^3$ [9] and MAMI $\alpha_\pi - \beta_\pi = (11.6 \pm 3.4) \cdot 10^{-4}\,\mathrm{fm}^3$ [10] which amount to values more than twice as large. Certainly, these existing experimental determinations of $\alpha_\pi - \beta_\pi$ raise doubts about their correctness since they violate the chiral low-energy theorem notably by a factor 2. The chiral low-energy theorem relates $\alpha_\pi - \beta_\pi = \alpha(\bar\ell_6 - \bar\ell_5)/(24\pi^2 f_\pi^2 m_\pi) + \mathcal{O}(m_\pi)$ to the axial-vector-to-vector form factor ratio $h_A/h_V = 0.443 \pm 0.015 = (\bar\ell_6 - \bar\ell_5)/6 + \mathcal{O}(m_\pi^2)$ measured in the PIBETA experiment [11] via the radiative pion decay $\pi^+ \to e^+\nu_e\gamma$. The two-loop calculations of refs. [8, 12, 13] assure that the $\mathcal{O}(m_\pi)$ corrections to $\alpha_\pi - \beta_\pi$ are in fact small. It is worth to note that a recent dispersive analysis [14] of the Belle data for $\gamma\gamma \to \pi^+\pi^-$ gives the fit value $\alpha_\pi - \beta_\pi = 4.7 \cdot 10^{-4}\,\mathrm{fm}^3$, compatible with the prediction of chiral perturbation theory. In a similar work by Hoferichter et al. [15] the complete system of Roy-Steiner equations for $\gamma\gamma \to \pi\pi$ and the crossed channel $\gamma\pi \to \gamma\pi$ has been solved. These integral equations fully respect analyticity, unitarity and crossing symmetry of the scattering amplitudes.

In that controversial situation, it is promising that the ongoing COMPASS experiment at CERN aims at measuring the pion polarizabilities, α_π and β_π, with high statistics using the Primakoff effect. The scattering of high-energy negative pions in the Coulomb field of a heavy nucleus (of charge Z) gives access to cross sections for $\pi^-\gamma$ reactions through the equivalent photon method:

$$\frac{d\sigma}{ds\,dQ^2} = \frac{Z^2\alpha}{\pi(s-m_\pi^2)}\,\frac{Q^2 - Q^2_{\mathrm{min}}}{Q^4}\,\sigma_{\pi^-\gamma}(s)\,, \qquad Q_{\mathrm{min}} = \frac{s-m_\pi^2}{2E_{\mathrm{beam}}}\,. \tag{1}$$

Here, Q denotes the momentum transferred by the virtual photon to the heavy nucleus of charge Z, and one aims at isolating the Coulomb peak $Q \to 0$ from the strong interaction background. The last factor $\sigma_{\pi^-\gamma}(s)$ is the total cross section for a $\pi^-\gamma$ reaction induced by real photons with $\sqrt{s}$ the corresponding $\pi^-\gamma$ center-of-mass energy. Note that eq.(1) applies in the same form to differential cross sections on both sides. The COMPASS experiment is set up to detect simultaneously various (multi-particle) hadronic final states which are produced in the Primakoff scattering process of high-energy pions. In addition to pion Compton scattering $\pi^-\gamma \to \pi^-\gamma$ (which is of primary interest for determining the pion polarizabilities α_π and β_π) the reaction $\pi^-\gamma \to \pi^-\pi^0$ serves as a test of the QCD chiral anomaly (i.e. the anomalous $VAAA$ rectangle quark diagram) by measuring the $\gamma 3\pi$ coupling constant $F_{\gamma 3\pi} = e/(4\pi^2 f_\pi^3) = 9.72\,\mathrm{GeV}^{-3}$. For the two-body process $\pi^-\gamma \to \pi^-\pi^0$ the one-loop [16, 17] and two-loop corrections [18] of chiral perturbation theory as well as QED radiative corrections [19] have been worked out. Thus an accurate theoretical framework is available to analyze the upcoming data. The consistent theoretical framework to extract the pion polarizabilities from the measured cross sections for (low-energy) pion-Compton scattering $\pi^-\gamma \to \pi^-\gamma$ or the primary pion-nucleus bremsstrahlung process $\pi^- Z \to \pi^- Z\gamma$ has been described (in one-loop approximation) in refs. [17, 20]. It has been stressed that at the same order as the pion polarizability difference $\alpha_\pi - \beta_\pi$ there exists a further (partly compensating) pion structure effect in form of a unique pion-loop correction (interpretable as photon scattering off the "pion-cloud around the pion"). In addition to these strong interaction effects, the QED radiative corrections to real and virtual pion Compton scattering $\pi^-\gamma^{(*)} \to \pi^-\gamma$ have been calculated in refs. [20, 21]. The relative smallness of the pion structure effects in low-energy pion Compton scattering makes it necessary to include these higher order electromagnetic corrections.

The $\pi^-\gamma$ reaction with three charged pions in the final state is used by the COMPASS collaboration in the energy range $1\,\mathrm{GeV} < \sqrt{s} < 2.5\,\mathrm{GeV}$ to study the spectroscopy of non-strange meson resonances ($a_1(1260)$, $a_2(1320)$, $\pi_2(1670)$, etc.) and to search for so-called exotic meson resonances [22] (e.g. $\pi_1(1600)$) with quantum numbers different from simple (constituent) quark-antiquark bound states. The statistics of the COMPASS experiment is actually so high that the event rates with three pions in the final state can even be continued downward to the threshold. The cross sections (and other more exclusive observables) of the $\pi^-\gamma \to 3\pi$ reactions in the low-energy region $\sqrt{s} < 1\,\mathrm{GeV}$ offer new possibilities to test the strong interaction dynamics of pions as predicted by chiral perturbation theory. The total cross sections for the processes $\pi^-\gamma \to \pi^-\pi^0\pi^0$ and $\pi^-\gamma \to \pi^+\pi^-\pi^-$ have been calculated in ref. [17] at tree-level. Both reactions are governed (at leading order) by the chiral pion-pion interaction in combination with the electromagnetic photon-pion coupling. Clearly, in order to sharpen the predictions for $\pi^-\gamma \to 3\pi$ complete next-to-leading order calculations with inclusion of all corrections from pion-loops and chiral-invariant counterterms are necessary. In the neutral channel $\pi^-\gamma \to \pi^-\pi^0\pi^0$ it is found that the total cross sections (and two-pion mass spectra) get enhanced by a factor $1.5 - 1.8$ by the next-to-leading order corrections [23]. By contrast the cross sections for charged pion-pair production remain almost unchanged in comparison to their tree-level results. This different behavior can be understood from the varying influence of the chiral corrections on the pion-pion final-state interaction ($\pi^+\pi^- \to \pi^0\pi^0$ versus $\pi^-\pi^- \to \pi^-\pi^-$). In case of the cross sections for $\pi^-\gamma \to \pi^+\pi^-\pi^-$ in the near threshold region $\sqrt{s} < 5m_\pi$, a recent analysis of the COMPASS data nicely confirms the prediction of chiral perturbation theory (see herefore the contributions of S. Neubert and S. Grabmüller to these proceedings).

2 Charged Pion-Compton Scattering

Let us start with defining the invariant amplitudes for the pion Compton scattering process: $\pi^-(p_1) + \gamma(k_1, \epsilon_1) \to \pi^-(p_2) + \gamma(k_2, \epsilon_2)$. The corresponding T-matrix in the center-of-mass frame has (in Coulomb gauge $\epsilon^0_{1,2} = 0$) the form:

$$T_{\pi\gamma} = 8\pi\alpha\Big\{ -\vec{\epsilon}_1 \cdot \vec{\epsilon}_2^{\,*} \, A(s,t) + \vec{\epsilon}_1 \cdot \vec{k}_2 \, \vec{\epsilon}_2^{\,*} \cdot \vec{k}_1 \, \frac{2}{t} \Big[A(s,t) + B(s,t) \Big] \Big\} \,, \tag{2}$$

with $\alpha = 1/137.036$ the fine-structure constant, and $s = (p_1 + k_1)^2 > m_\pi^2$ and $t = (k_1 - k_2)^2 < 0$ the independent Mandelstam variables. $m_\pi = 139.57\,\text{MeV}$ denotes the charged pion mass. Performing the sums over transversal photon polarizations and applying the flux and phase space factors, the resulting differential cross section reads:

$$\frac{d\sigma}{d\Omega_{\text{cm}}} = \frac{\alpha^2}{2s} \Big\{ |A(s,t)|^2 + |A(s,t) + (1+z)B(s,t)|^2 \Big\} \,, \tag{3}$$

with $t = (s - m_\pi^2)^2(z-1)/2s$, where $z = \cos\theta_{\text{cm}} = \hat{k}_1 \cdot \hat{k}_2$ is the cosine of the cms scattering angle. The amplitudes at tree level coincide with those of scalar quantum electrodynamics:

$$A(s,t)^{(\text{tree})} = 1, \qquad B(s,t)^{(\text{tree})} = \frac{s - m_\pi^2}{m_\pi^2 - s - t} \,. \tag{4}$$

The one-pion loop diagrams of chiral perturbation theory generate, after renormalization of the pion mass, the following (finite) contribution to the Compton amplitude $A(s,t)$:

$$A(s,t)^{(\text{loop})} = \frac{1}{(4\pi f_\pi)^2} \left\{ -\frac{t}{2} - 2m_\pi^2 \ln^2 \frac{\sqrt{4m_\pi^2 - t} + \sqrt{-t}}{2m_\pi} \right\} , \tag{5}$$

where $f_\pi = 92.4\,\text{MeV}$ denotes the pion decay constant. This term can be interpreted as the (leading) correction arising from photon scattering off the "pion cloud around the pion". The internal structure of the pion enters through its electric and magnetic polarizabilities, which obey at one-loop order the constraint $\alpha_\pi + \beta_\pi = 0$. The pertinent $\gamma\gamma\pi\pi$ contact vertex from the chiral Lagrangian $\mathcal{L}^{(4)}_{\pi\pi}$ gives rise to the contribution

$$A(s,t)^{(\text{pola})} = -\frac{\beta_\pi m_\pi t}{2\alpha} < 0 \,, \qquad \alpha_\pi - \beta_\pi = \frac{\alpha(\bar{\ell}_6 - \bar{\ell}_5)}{24\pi^2 f_\pi^2 m_\pi} \,. \tag{6}$$

The combination of low-energy constants can be extracted from the axial-vector-to-vector form factor ratio $h_A/h_V = 0.443 \pm 0.015 = (\bar{\ell}_6 - \bar{\ell}_5)/6 + \mathcal{O}(m_\pi^2)$ measured in the PIBETA experiment [11] at PSI via the radiative pion decay $\pi^+ \to e^+\nu_e\gamma$. The two-loop analysis of ref. [13] yields the value $\bar{\ell}_6 - \bar{\ell}_5 = 3.0 \pm 0.3$, implying pion polarizabilities of magnitude $\alpha_\pi = -\beta_\pi \simeq 3.0 \cdot 10^{-4}\,\text{fm}^3$.

The effects of the pion structure on the differential Compton cross section are shown in Fig. 1. The reduction of $d\sigma/d\Omega_{\text{cm}}$ in backward directions ($z \simeq -1$) caused by the polarizability difference $\alpha_\pi - \beta_\pi$ gets in fact partly compensated by the pion-loop correction

$A(s,t)^{(\mathrm{loop})} \sim t^2 > 0$ written in eq.(5). In order to visualize more directly the effect of the pion polarizabilities, we show in Fig. 2 the ratio $d\sigma/d\sigma_0$ between the differential cross sections in backward direction, $z = -1$, calculated with finite, $\alpha_\pi = -\beta_\pi = 3.0 \cdot 10^{-4}\,\mathrm{fm}^3$, and with zero pion polarizabilities. At $\sqrt{s} = 4m_\pi$ the effect becomes now quite sizeable, where it amounts to almost a 20% reduction of the backward differential cross section. Let us also mention that these results receive only small corrections in a full two-loop description of pion Compton scattering [8]. At this order the predictions for the pion polarizability difference and sum are: $\alpha_\pi - \beta_\pi = (5.7 \pm 1.0) \cdot 10^{-4}\,\mathrm{fm}^3$ and $\alpha_\pi + \beta_\pi = (0.16 \pm 0.1) \cdot 10^{-4}\,\mathrm{fm}^3$. Isospin breaking corrections to pion Compton scattering arising from the mass difference of the charged and neutral pion (which is mainly of electromagnetic origin) have been considered in ref. [24]. The effects on the Compton cross section turn out to be negligibly small, i.e. they are of the order of just a few permille.

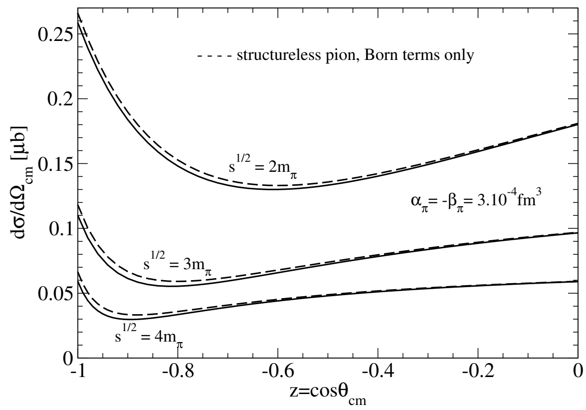

Figure 1: Differential cross section for pion Compton scattering.

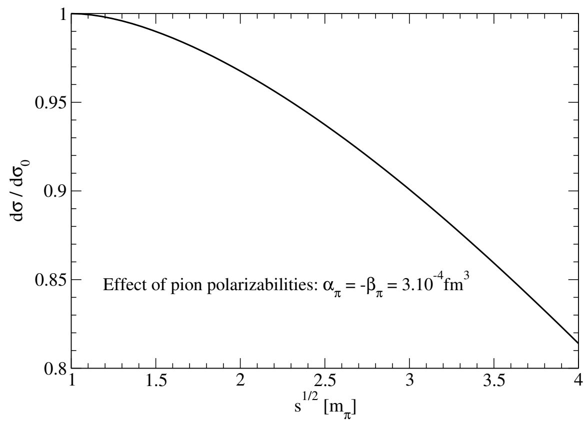

Figure 2: Ratio $d\sigma/d\sigma_0$ between differential cross sections in backward direction ($z = -1$) calculated with finite, $\alpha_\pi = -\beta_\pi = 3.0 \cdot 10^{-4}\,\mathrm{fm}^3$, and with zero pion polarizabilities.

3 Radiative Corrections

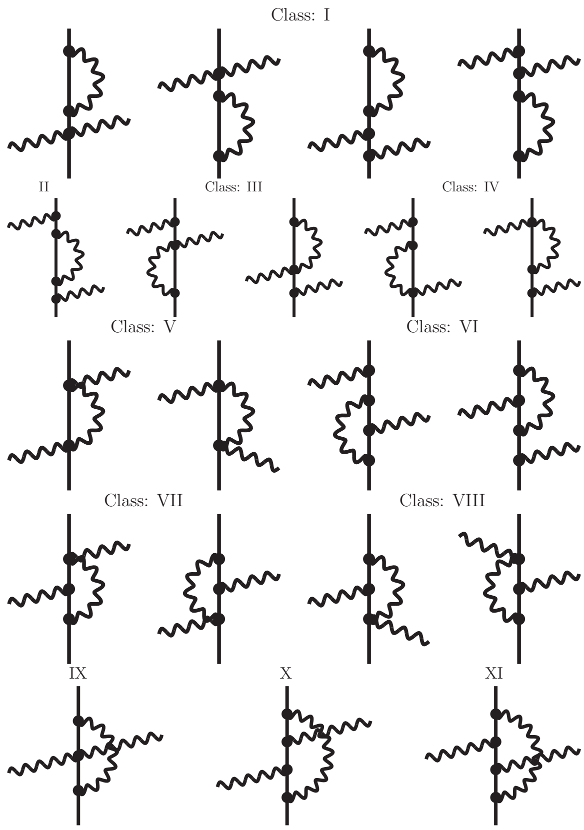

Figure 3: One-photon loop diagrams for pion Compton scattering

The relative smallness of the pion structure effects in Compton scattering makes it necessary to consider also higher order electromagnetic corrections arising from photon loops and soft photon bremsstrahlung. The pertinent one-photon loop diagrams are shown in Fig. 3. The analytical expressions for the loop amplitudes $A(s,t)$ and $B(s,t)$ of order α are given in section 3 of ref. [20]. Since scalar QED is a renormalizable quantum field theory ultraviolet divergent terms drop out in the total sum of all diagrams. Infrared finiteness of the virtual radiative corrections is achieved (in the standard way) by including soft radiation below an energy cut-off λ. In its final effect, the (single) soft photon radiation off the in- or out-going pion multiplies the tree-level differential cross section $d\sigma/d\Omega$ by a factor:

$$\delta_{\text{soft}} = \alpha\mu \int\limits_{|\vec{l}\,|<\lambda} \frac{d^{d-1}l}{(2\pi)^{d-2}l_0} \left\{ \frac{2m_\pi^2 - t}{p_1 \cdot l\, p_2 \cdot l} - \frac{m_\pi^2}{(p_1 \cdot l)^2} - \frac{m_\pi^2}{(p_2 \cdot l)^2} \right\}, \tag{7}$$

which exactly cancels the infrared divergent terms generated by the photon loops (proportional to $\xi_{\text{IR}} = 1/(d-4) + (\gamma_E - \ln 4\pi)/2 + \ln(m_\pi/\mu)$ in dimensional regularization).

The sum of virtual and real radiative corrections to pion Compton scattering is shown in Fig. 4 at selected center-of-mass energies $\sqrt{s} = (2, 3, 4, 5)m_\pi$ as a function of $z = \cos\theta_{\rm cm}$. The detection threshold for soft photons has been set to the value $\lambda = 5\,\mathrm{MeV}$. One observes that the radiative corrections grow with the center-of-mass energy and that they become maximal in backward directions $z \simeq -1$, reaching values up to -2.4% at $\sqrt{s} = 4m_\pi$. With such an angular dependence the pure QED radiative corrections have the same kinematical signature as the effects from the pion's low-energy structure (i.e. pion polarizability difference plus pion-loop correction). In magnitude they are still suppressed by a factor $5 - 10$. A proper inclusion of radiative corrections is therefore essential if one wants to extract the pion polarizabilities with good accuracy. In the calculation of radiative corrections the leading pion structure can be accounted for by interpreting one of the two-photon contact vertices in the photon-loop diagrams as the polarizability vertex proportional to $\beta_\pi m_\pi$. As one can see from Fig. 5 such an improved description leaves the size and angular dependence of the radiative corrections practically unchanged.

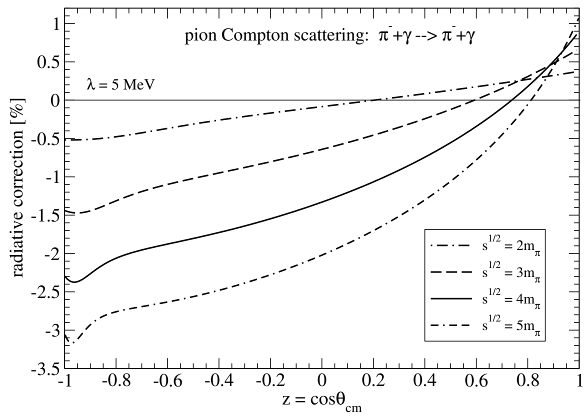

Figure 4: Radiative corrections to pion Compton scattering. The pion is treated as a structureless spin-0 boson.

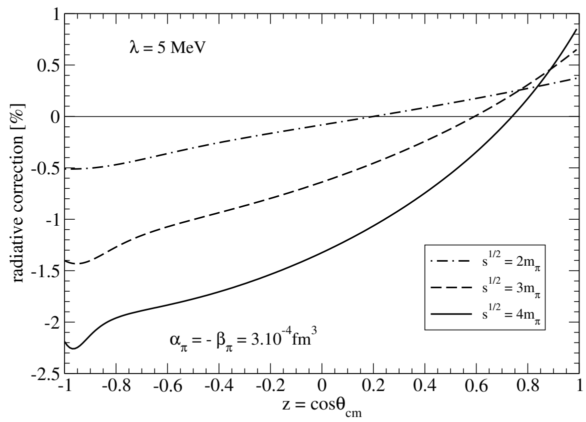

Figure 5: Radiative corrections to pion Compton scattering taking into account the polarizability difference $\alpha_\pi - \beta_\pi \simeq 6.0 \cdot 10^{-4}\,\mathrm{fm}^3$.

4 Neutral Pion-Pair Production

In this section we treat the neutral pion-pair production process $\pi^-(p_1) + \gamma(k, \epsilon) \to \pi^-(p_2) + \pi^0(q_1) + \pi^0(q_2)$. The general form of the T-matrix reads (in Coulomb-gauge):

$$T = \frac{2e}{f_\pi^2}\Big[\vec{\epsilon}\cdot\vec{q}_1\, A_1 + \vec{\epsilon}\cdot\vec{q}_2\, A_2\Big]\,. \tag{8}$$

In this decomposition A_1 and A_2 are two dimensionless production amplitudes which depend on $s = (p_1 + k)^2$ and four other independent Lorentz-invariant variables:

$$s_1 = (p_2 + q_1)^2\,, \quad s_2 = (p_2 + q_2)^2\,, \quad t_1 = (q_1 - k)^2\,, \quad t_2 = (q_2 - k)^2\,. \tag{9}$$

This set is very convenient for describing the permutation of the two identical neutral pions in the final state via $(s_1 \leftrightarrow s_2,\ t_1 \leftrightarrow t_2)$. The tree diagrams of chiral perturbation theory for the processes $\pi^-\gamma \to 3\pi$ are shown in Fig. 6. In the case of neutral pion-pair production only the left diagram contributes. In terms of the kinematical variables introduced in eq.(9) the tree-level amplitudes read:

$$A_1^{(\mathrm{tree})} = A_2^{(\mathrm{tree})} = \frac{2m_\pi^2 + s - s_1 - s_2}{3m_\pi^2 - s - t_1 - t_2}\,. \tag{10}$$

In this expression the numerator comes from the chiral $\pi^+\pi^- \to \pi^0\pi^0$ interaction and the denominator from the propagator of outgoing π^- to which the (real) photon couples.

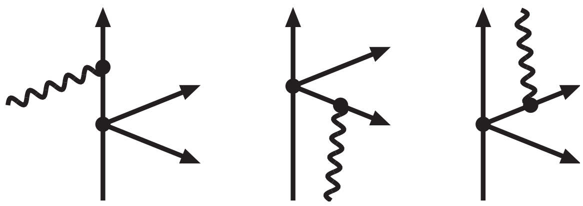

Figure 6: Tree diagrams for $\pi^-\gamma \to \pi^-\pi^0\pi^0$ and $\pi^+\pi^-\pi^-$. Arrows indicate outgoing pions. Only the left diagram contributes to $2\pi^0$-production.

The next-to-leading order corrections arise from pion-loop diagrams and chiral-invariant counterterms involving the low-energy constants $\bar{\ell}_1, \bar{\ell}_2, \bar{\ell}_3$ and $\bar{\ell}_4$. The analytical expressions for the pertinent production amplitudes A_1 and A_2 are given for individual diagrams in section 2.1 of ref. [23]. The total cross section is obtained by integrating the squared (transversal) T-matrix over the three-pion phase space:

$$\sigma_{\mathrm{tot}}(s) = \frac{\alpha}{32\pi^3 f_\pi^4 (s - m_\pi^2)} \iint\limits_{z^2<1} d\omega_1 d\omega_2 \int_{-1}^{1} dx \int_0^\pi d\phi \left|\hat{k} \times (\vec{q}_1 A_1 + \vec{q}_2 A_2)\right|^2 . \tag{11}$$

Fig. 7 shows the total cross section $\sigma_{\rm tot}(s)$ for the reaction $\pi^-\gamma \to \pi^-\pi^0\pi^0$ in the low-energy region from threshold $\sqrt{s} = 3m_\pi$ up to $\sqrt{s} = 7m_\pi$. The dashed line corresponds to the tree approximation and the full line includes in addition the next-to-leading order corrections from chiral loops and counterterms. We use for the low-energy constants $\bar{\ell}_j$ the values: $\bar{\ell}_1 = -0.4 \pm 0.6$, $\bar{\ell}_2 = 4.3 \pm 0.1$, $\bar{\ell}_3 = 2.9 \pm 2.4$, $\bar{\ell}_4 = 4.4 \pm 0.2$, as determined (with improved empirical input) in ref. [1] from $\pi\pi$-scattering data. One observes that the total cross section gets enhanced sizeably (by a factor of $1.5 - 1.8$) after the inclusion of the next-to-leading order chiral corrections. Although the dynamics of the whole process is much richer this feature can be understood (in an approximate way) from the $\pi^+\pi^- \to \pi^0\pi^0$ final state interaction. The $\pi^+\pi^- \to \pi^0\pi^0$ interaction strength at threshold is determined by the difference of the isospin-zero and isospin-two S-wave $\pi\pi$-scattering lengths. Considering the corresponding one-loop expression

$$\frac{1}{3}(a_0 - a_2) = \frac{3m_\pi}{32\pi f_\pi^2}\left[1 + \frac{m_\pi^2}{36\pi^2 f_\pi^2}\left(\bar{\ell}_1 + 2\bar{\ell}_2 - \frac{3\bar{\ell}_3}{8} + \frac{9\bar{\ell}_4}{2} + \frac{33}{8}\right)\right], \tag{12}$$

one finds that the correction to 1 inside the square bracket amounts to about 0.20 (inserting the central values of $\bar{\ell}_j$). The square of this number is in fact close to the enhancement factor of the total cross section. It is also important to investigate the uncertainties induced by the present errorbars of the low-energy constants $\bar{\ell}_j$. Taking the total cross section at $\sqrt{s} = 6m_\pi$ as a measure one finds a relative uncertainty of about $\pm 5.4\%$ which is mainly connected with the errorbar of $\bar{\ell}_1 = -0.4 \pm 0.6$. It is comforting that the badly known low-energy constant $\bar{\ell}_3 = 2.9 \pm 2.4$ has very little influence on the observables considered here. Altogether this amounts to a fairly accurate prediction which presumably can be trusted up to center-of-mass energies of $\sqrt{s} \simeq 6m_\pi$.

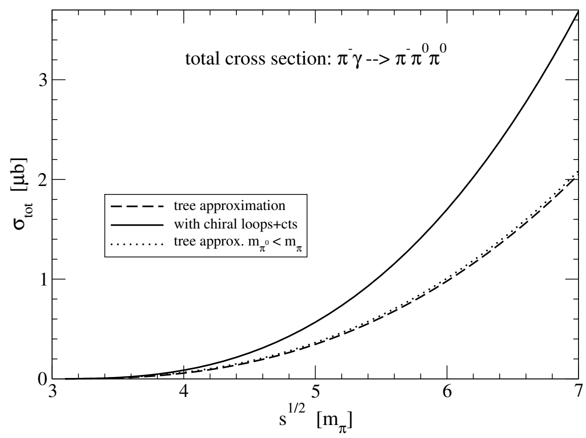

Figure 7: Total cross sections for neutral pion-pair production.

The radiative corrections to the process $\pi^-\gamma \to \pi^-\pi^0\pi^0$ have been calculated recently in ref. [25]. In this case only about a dozen photon-loop diagrams contribute and the radiative corrections can be represented by an overall correction factor, $R \sim \alpha/2\pi$, which multiplies the tree-level amplitude. The various contributions from photon-loops and soft photon bremsstrahlung to the total cross section are shown in Fig. 8. From threshold up to cms energies of $\sqrt{s} = 7m_\pi$ these radiative corrections are small and vary from $+1.6\%$ to -1.6%.

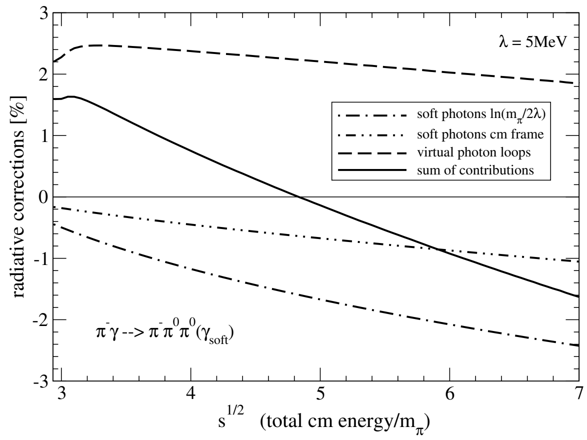

Figure 8: Radiative corrections to neutral pion-pair production.

5 Charged Pion-Pair Production

Finally, we discuss the charged pion-pair production process $\pi^-(p_1) + \gamma(k, \epsilon) \to \pi^+(p_2) + \pi^-(q_1) + \pi^-(q_2)$. By assigning the four-momentum p_2 to the out-going positively charged pion $\pi^+(p_2)$ one can exploit the complete equivalence to the $\pi^-\gamma \to \pi^-\pi^0\pi^0$ reaction concerning its kinematical description. The T-matrix (in Coulomb-gauge) and the Mandelstam variables are the same as defined in eqs.(8,9). The three non-vanishing tree diagrams shown in Fig. 6 lead to the following tree-level amplitudes:

$$A_1^{(\text{tree})} = \frac{s + m_\pi^2 - s_1 - s_2}{3m_\pi^2 - s - t_1 - t_2} + \frac{s - s_1 - s_2 + t_2}{t_1 - m_\pi^2} - 1\,, \tag{13}$$

$$A_2^{(\text{tree})} = \frac{s + m_\pi^2 - s_1 - s_2}{3m_\pi^2 - s - t_1 - t_2} + \frac{s - s_1 - s_2 + t_1}{t_2 - m_\pi^2} - 1\,. \tag{14}$$

Beyond leading order the dynamical content of charged pion-pair production $\pi^-\gamma \to \pi^+\pi^-\pi^-$ is considerably more extensive than that of neutral pion-pair production $\pi^-\gamma \to \pi^-\pi^0\pi^0$ because the photon can now couple to all three out-going (charged) pions. Many more diagrams with pion-loops and chiral counterterms do contribute. These diagrams have all been evaluated in section 3.1 of ref. [23]. Using consistently the same values of the low-energy constants $\bar{\ell}_1$, $\bar{\ell}_2$, $\bar{\ell}_3$ and $\bar{\ell}_4$ the result for the total cross section (computed via eq.(11)) follows as shown in Fig. 9. As a striking feature one observes that the total cross section for $\pi^-\gamma \to \pi^+\pi^-\pi^-$ remains almost unchanged in the region $\sqrt{s} < 6m_\pi$ after inclusion of the next-to-leading order chiral corrections. Although the dynamics of the whole process is much richer this can be understood (in a suggestive way) from the

$\pi^-\pi^- \to \pi^-\pi^-$ final state interaction. By considering the one-loop expression for the isospin-two S-wave $\pi\pi$-scattering length

$$a_2 = -\frac{m_\pi}{16\pi f_\pi^2}\left[1 - \frac{m_\pi^2}{12\pi^2 f_\pi^2}\left(\bar{\ell}_1 + 2\bar{\ell}_2 - \frac{3\bar{\ell}_3}{8} - \frac{3\bar{\ell}_4}{2} + \frac{3}{8}\right)\right], \tag{15}$$

one deduces that the correction to 1 inside the square bracket amounts to a very small number. Chiral corrections (even at two-loop order [1]) affect the isospin-two $\pi\pi$-interaction only very weakly and this feature seems to be reflected by $\sigma_{\rm tot}(s)$ in Fig. 9. A recent analysis of the COMPASS data in the region $\sqrt{s} < 5m_\pi$ confirms the prediction of chiral perturbation theory (see the contributions of S. Neubert and S. Grabmüller to these proceedings).

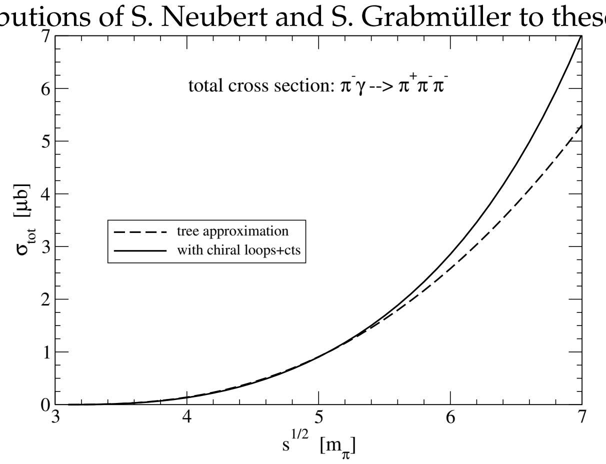

Figure 9: Total cross sections for charged pion-pair production.

The $\pi^+\pi^-$ mass spectra in Fig. 10 also show some interesting structures. The dip at intermediate $\pi^+\pi^-$ masses is a manifestation of chiral pion-loop dynamics. It is expected that the high-statistics data of the COMPASS experiment can reveal such dynamical details.

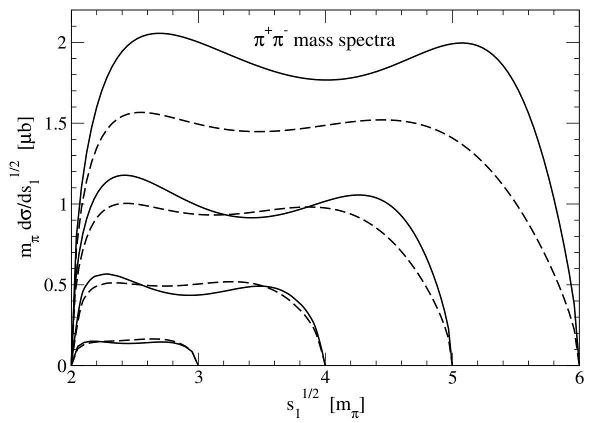

Figure 10: $\pi^+\pi^-$ mass spectra for the reaction $\pi^-\gamma \to \pi^+\pi^-\pi^-$.

Acknowledgments

I thank the organizers for invitation to the conference HADRON2011. I thank Jan Friedrich for many informative discussions and fruitful collaboration over the past years.

References

[1] G. Colangelo, J. Gasser, and H. Leutwyler, *Nucl. Phys.* **B603**, 125 (2001).

[2] S. Pislak et al., *Phys. Rev.* **D67**, 072004 (2003).

[3] J.R. Batley et al., *Eur. Phys. J.* **C54**, 411 (2008).

[4] G. Colangelo, J. Gasser, and H. Leutwyler, *Phys. Rev. Lett.* **86**, 5008 (2001).

[5] B. Adeva et al., *J. Phys.* **G30**, 1929 (2004).

[6] J.R. Batley et al., *Eur. Phys. J.* **C64**, 589 (2009).

[7] M. Bissegger, A. Fuhrer, J. Gasser, B. Kubis, and A. Rusetsky, *Nucl. Phys.* **B 806**, 178 (2009); G. Colangelo, J. Gasser, and A. Rusetsky, *Eur. Phys. J.* **C59**, 777 (2009).

[8] J. Gasser, M.A. Ivanov, and M.E. Sainio, *Nucl. Phys.* **B745**, 84 (2006); and private communications.

[9] Y.M. Antipov et al., *Phys. Lett.* **B121**, 445 (1983); *Z. Phys.* **C26**, 495 (1985).

[10] J. Ahrens et al., *Eur. Phys. J.* **A23**, 113 (2005).

[11] E. Frlez et al., *Phys. Rev. Lett.* **93**, 181804 (2004); E. Frlez, *Nucl. Phys. Proc. Suppl.* **162**, 148 (2006).

[12] U. Bürgi, *Phys. Lett.* **B377**, 147 (1996); *Nucl. Phys.* **B479**, 392 (1996).

[13] J. Bijnens and P. Talavera, *Nucl. Phys.* **B489**, 387 (1997);
C.Q. Geng, I.L. Ho, and T.H. Wu, *Nucl. Phys.* **B684**, 2815 (2004).

[14] R. Garcia-Martin and B. Moussallam, *Eur. Phys. J.* **C70** 155 (2010).

[15] M. Hoferichter, D.R. Philips, and C. Schat, hep-ph/1106.4147.

[16] J. Bijnens, A. Bramon, and F. Cornet, *Phys. Lett.* **B237**, 488 (1990);
J. Bijnens, *Int. J. Mod. Phys.* **A8**, 3045 (1993).

[17] N. Kaiser and J.M. Friedrich, *Eur. Phys. J.* **A36**, 181 (2008).

[18] T. Hannah, *Nucl. Phys.* **B593**, 577 (2001).

[19] L. Ametller, M. Knecht, and P. Talavera, *Phys. Rev.* **D64**, 094009 (2001).

[20] N. Kaiser and J.M. Friedrich, *Nucl. Phys.* **A812**, 186 (2008).

[21] N. Kaiser and J.M. Friedrich, *Eur. Phys. J.* **A39**, 71 (2008).

[22] COMPASS collaboration: M.G. Alekseev et al., *Phys. Rev. Lett.* **104**, 241803 (2010).

[23] N. Kaiser, *Nucl. Phys.* **A848**, 198 (2010).

[24] N. Kaiser, *Eur. Phys. J.* **A47**, 15 (2011).

[25] N. Kaiser, *Eur. Phys. J.* **A46**, 373 (2010).